Pedosphere **36**(2): 554–567, 2026
doi: 10.1016/j.pedsph.2024.11.004
ISSN 1002-0160/CN 32-1315/P
© 2026 Soil Science Society of China
Published by Elsevier B.V. and Science Press

PEDOSPHERE

www.elsevier.com/locate/pedosphere

Impact of organic carbon composition on bacterial community assembly in organic and mineral soil layers under phosphorus addition in a *Robinia pseudoacacia* plantation

Ahejiang SAILIKE[1], Yujie LIANG[1], Rong FU[1], Hongjian HAO[1], Rong WANG[1], Ning PENG[2], Shicai LI[1], Zhouchang YU[1], Fangxin ZHENG[1], Wei ZHANG[1,*], Yangyang LIU[1,*], Peizhi YANG[1] and Zhixin ZHANG[1]

[1]*College of Grassland Agriculture, Northwest A&F University, Yangling 712100 (China)*
[2]*College of Life Sciences, Northwest A&F University, Yangling 712100 (China)*

(Received September 12, 2024; revised October 23, 2024; accepted October 31, 2024)

ABSTRACT

Increasing phosphorus (P) inputs significantly affect the nutrient cycle of terrestrial ecosystems. The community structure and assembly processes of soil bacteria, which are the primary participants in nutrient cycling within terrestrial ecosystems, are affected by P inputs. However, the assembly processes and driving mechanisms of soil bacterial communities in artificial forest ecosystems in response to P inputs remain unclear. Therefore, in this study, an experiment was conducted in an artificial *Robinia pseudoacacia* forest on the Loess Plateau to investigate the effects of P additions (0, 0.5, 1, 2, and 4 g P m^{-2} $year^{-1}$) on soil organic carbon (SOC) composition, bacterial community characteristics (total, abundant, and rare taxa), and assembly processes in the organic horizon (OH) and mineral horizon (MH). The results showed that P addition significantly changed soil physicochemical properties, such as available P (AP), SOC content, and SOC composition in terms of labile and recalcitrant SOC fractions. The proportion of labile SOC fraction increased in OH and decreased in MH, whereas the recalcitrant SOC fraction showed the opposite trend. In OH, the proportion of eutrophic bacteria increased, whereas the proportion of oligotrophic bacteria decreased. In contrast to those in OH, the changes in eutrophic and oligotrophic bacteria in MH exhibited the opposite trend. The diversity of bacterial communities in OH did not change significantly with increasing P levels. In MH, the diversity of total and rare taxa increased, while the diversity of abundant taxa decreased. Under P addition, the total and rare bacterial taxa showed stochastic assembly, whereas the assembly of abundant taxa shifted from stochastic to deterministic processes in OH and from deterministic to stochastic processes in MH. The partial-least squares path modeling revealed that under P addition, the assembly of total and rare bacterial communities in OH and MH was regulated by AP and labile SOC fraction, respectively. Meanwhile, the assembly of abundant taxa in OH and MH was influenced by labile and recalcitrant SOC fractions, respectively. Our findings highlight the critical role of SOC composition across different bacterial taxa, with abundant taxa exhibiting heightened sensitivity to environmental filtration and the availability of SOC resources. Our study provides new insights into the community assembly and driving mechanisms of soil bacteria in artificial forest soils under P addition.

Key Words: abundant taxa, afforestation, artificial forest, bacterial community assembly, mineral horizon, organic horizon, rare taxa, soil organic C

Citation: Sailike A, Liang Y J, Fu R, Hao H J, Wang R, Peng N, Li S C, Yu Z C, Zheng F X, Zhang W, Liu Y Y, Yang P Z, Zhang Z X. 2026. Impact of organic carbon composition on bacterial community assembly in organic and mineral soil layers under phosphorus addition in a *Robinia pseudoacacia* plantation. *Pedosphere*. **36**(2): 554–567.

INTRODUCTION

In recent years, increased phosphorus (P) inputs due to human activities have substantially raised P availability in soils (Peñuelas *et al*., 2013, 2020). Increased P availability in soil promotes plant growth, enhancing nutrient return from litter and inducing changes in soil organic carbon (SOC) (Yue *et al*., 2017; Gong *et al*., 2023; Wang *et al*., 2023). Since P is an essential element for bacterial growth and development, and SOC serves as a resource for soil bacteria, the changes in SOC resulting from altered soil P levels can regulate the shifts in bacterial community structure and assembly processes in soil (Sun *et al*., 2022; Wu *et al*., 2023). However, uncertainties still exist regarding how P addition affects SOC and how both factors impact bacterial community assembly, limiting our understanding of how bacterial communities mediate nutrient cycling under P addition.

By affecting plant growth, P addition can influence SOC dynamics (Sun *et al*., 2022; Gong *et al*., 2023). For example, Feng *et al*. (2023) found that P addition promoted plant growth, resulting in more litter and root residue, and increased the SOC content. However, other studies reported that P addition decreased the SOC content by enhancing microbial activity and promoting SOC decomposition (Luo *et al*., 2020; Li *et al*., 2021). Traditionally, the variability in the response of SOC to P addition is attributed to the differences in vegetation type and experimental condition (Jiang *et al*., 2021). Recent studies, however, have highlighted the influence of P addition on SOC dynamics in different soil

*Corresponding author. E-mail: zwgwyd@163.com, hnlylcbtks@163.com.

layers (Hou *et al*., 2020; Huang *et al*., 2021; Zhao *et al*., 2022). For example, in a subalpine forest ecosystem, under the same P application method using NaH_2PO_4, P addition at 5–30 g P m^{-2} $year^{-1}$ reduced plant carbon (C) allocation to belowground biomass, which led to decreased root residue accumulation and subsequently resulted in a decline in the SOC content in the mineral horizon (MH, 3–10 cm) (Luo *et al*., 2022). In contrast, in an alpine meadow ecosystem, P addition at 5–15 g P m^{-2} $year^{-1}$ increased the SOC content in the organic horizon (OH, 0–3 cm), but simultaneously reduced the SOC content in MH by accelerating the decomposition of recalcitrant SOC (Ma *et al*., 2023). These contrasting findings suggest that the influence of P addition on SOC in different soil layers remains uncertain owing to the complexity of C composition and the diversity of influencing factors (Fontaine *et al*., 2007; Wang *et al*., 2017; Shi *et al*., 2023). Additionally, these uncertainties may arise from the focus on natural ecosystems, with insufficient research on artificial ecosystems that are characterized by simplified vegetation structures and greater human disturbance (Zhong *et al*., 2020). Therefore, detailed research on the responses of SOC and its composition to P addition in different soil layers in artificial ecosystems can help elucidate the impact of P addition on SOC.

Bacteria, the most abundant microbial species in soil, play a critical role in nutrient cycling, particularly in SOC decomposition, compared to soil fungi and archaea (Kennedy, 1999; Khan *et al*., 2016; Wang *et al*., 2019; Qin *et al*., 2020). Bacterial community assembly can help effectively assess the mechanisms of community formation and maintenance (Chase, 2010; Yan *et al*., 2019; Chen and Xiao, 2023). However, P, an essential element for bacterial growth, affects the growth and development of different bacterial taxa and their community assembly processes (Peng *et al*., 2021; Chen and Xiao, 2023). Studies have shown that P addition causes stochastic processes to dominate community assembly, with abundant bacterial taxa undergoing homogeneous selection and undominated processes (Shi *et al*., 2020; Wu *et al*., 2023). However, as P effectiveness and level increase, the proportion of deterministic processes in community assembly also rises (Yu *et al*., 2019). Therefore, the effects of P addition on the relative importance of deterministic and stochastic processes are inconsistent. Previous studies have indicated that this inconsistency is determined by soil physicochemical properties, such as available nutrients (Yu *et al*., 2019). Other studies have inferred that the uncertainty in community assembly under P addition may also stem from the changes in SOC (Zhu *et al*., 2020; Ling *et al*., 2021), as SOC serves as a resource for bacteria and plays a key role in regulating bacterial community assembly (Huang *et al*., 2022). During ecological succession, the labile SOC fraction drives bacterial community assembly by influencing bacterial diversity and keystone taxa (Shi *et al*., 2023). Additionally, the recalcitrant SOC fraction drives community assembly by altering the composition of bacterial communities (Zhang *et al*., 2022). Although SOC and its composition have been found to affect bacterial community assembly, there is limited research on whether P addition influences bacterial community assembly by altering SOC and its composition. In particular, the manner through which the changes in SOC and its composition induced by P addition drive bacterial community assembly in different soil layers remains unknown. Understanding this is crucial for uncovering the regulatory mechanisms by which P addition affects soil bacterial community composition and diversity.

The "Returning Farmland to Forest" Project has been implemented for many years in the Loess Plateau region, China. *Robinia pseudoacacia* (RP), with its unique biological characteristics such as drought resistance and adaptability to poor soil, is a suitable pioneer tree species for afforestation in the Loess Plateau, playing a crucial role in improving the ecological environment (Zhang *et al*., 2018). Numerous studies have examined the characteristics of RP, soil properties, and microbial communities (Zhang *et al*., 2019; Xu *et al*., 2020; Su and Shangguan, 2021). However, few studies have investigated the effects of P addition on SOC and its composition in RP plantations, especially on the responses of bacterial community assembly across different soil layers to the changes in SOC composition induced by P addition. Therefore, in this study, we aimed to determine the key factors affecting SOC composition changes in RP plantations under P addition and the driving factors behind the assembly processes of different bacterial taxa. A field experiment with P addition was conducted to simulate P inputs, during which soil physicochemical properties, SOC content and its composition, enzyme activities, and the compositions of abundant and rare taxa of bacterial communities were measured in OH and MH. We explored the effects of P addition on SOC and its composition, focusing on how these changes influenced the assembly processes of different bacterial taxa. We hypothesized that 1) P addition increases SOC and alters SOC composition in OH and MH; 2) P addition shifts the assembly of abundant taxa from stochastic to deterministic processes in OH, with the opposite trend in MH; and 3) the responses of available P (AP) and SOC components in different soil layers to P addition can explain the changes in bacterial community structure and assembly processes. The results of this study will provide valuable insights for optimizing strategies for sustainable forest management.

MATERIALS AND METHODS

Study area

The experiment was conducted in an artificial RP forest located on the Loess Plateau in the Wuliwan watershed of

Ansai District, Shaanxi Province, China (36°51′–36°53′ N, 109°20′–109°22′ E, 997–1 131 m above sea level). The region experiences a warm temperate semi-arid continental monsoon climate, with an average annual rainfall of 505 mm concentrated from July to September. The average annual temperature is 8.9 °C, and the annual sunshine duration ranges from 2 000 to 3 100 h. The soil type is yellow loam, derived from loess parent material, characterized by poor fertility, a loose texture, and low erosion resistance. The dominant artificial vegetation in the region consists of RP forests, which play a key role in soil and water conservation and ecological restoration (Deng *et al*., 2016; Su and Shangguan, 2021).

Experimental design and sampling

Based on the data from the local forestry department, we selected a 30-year-old artificial RP forest with uniform planting density as the experimental site. The experiment commenced in March 2018, using a one-way completely randomized block design for P addition. Each experimental plot measured 5 m × 5 m, with a 5 m gap horizontally and a 7 m gap vertically between the plots. To prevent the influence of surface runoff, a spacer with a height of 30 cm was inserted into each plot (Fig. S1, see Supplementary Material for Fig. S1). This study included five treatments, with P addition at 0.5 (P1), 1 (P2), 2 (P3), and 4 (P4) g P m^{-2} $year^{-1}$ and with no P addition (control, CK), with each treatment replicated three times. In each year P addition was performed four times, with 1/6, 1/3, 1/3, and 1/6 of the total amount added in March, June, September, and December, respectively. A mixture of KH_2PO_4 and KCl was used, wherein the addition of KCl balanced the potassium ions in KH_2PO_4, which was subsequently dissolved in 2 L of water and sprayed uniformly onto the soil surface of the understory. To eliminate differences in soil moisture content, the control plots were sprayed with equal amounts of water.

During the peak growth season of RP in August 2022, specific sampling procedures were implemented, and surface litter was removed from each plot. Subsequently, a five-point sampling method was employed to collect soil samples from OH and MH at depths of 0–3 and 3–10 cm, respectively, after the removal of visible plant roots, stones, debris, and fragments. The collected soil samples were thoroughly mixed and immediately sieved through a 2-mm mesh sieve. A total of 30 soil samples (five treatments × three replicates × two soil layers) were collected. The samples were then divided into three parts: one part was air-dried for analying soil physicochemical properties and related indicators of SOC components, the other was stored at 4 °C for the determination of enzyme activities, and the third was preserved at −80 °C for DNA extraction.

Determination of soil physicochemical properties and SOC components

Soil pH was measured at a soil-to-water ratio of 1:2.5 (weight:weight) with a pH meter (PHS-3C, Shanghai INESA Scientific Instrument Co., Ltd., China). The total nitrogen (TN) and total P (TP) contents in the soil were determined using wet digestion with K_2SO_4:$CuSO_4{\cdot}5H_2O$ (10:1, weight: weight)-H_2SO_4 and $HClO_4$-H_2SO_4, respectively (Zhang *et al*., 2019). Soil ammonium nitrogen (NH_4^+-N) and nitrate nitrogen (NO_3^--N) were extracted using 1 mol L^{-1} KCl, whereas soil AP was extracted using 0.5 mol L^{-1} $NaHCO_3$ (Jones and Willett, 2006; Zhang *et al*., 2019; Yu *et al*., 2023). All measurements were conducted using an Auto Analyzer 3 (Seal Analytical, Germany). The activities of soil extracellular enzymes, including β-1,4-glucosidase (βG), alkaline phosphatase (ALP), cellobiohydrolase (CBH), and β-1,4-*N*-acetylglucosaminidase (NAG), were determined using the microplate fluorescence method (Paz-Ferreiro *et al*., 2012; Xu *et al*., 2022; Hao *et al*., 2024).

The SOC content was determined using the $K_2Cr_2O_7$-H_2SO_4 method with additional heat capacity (Liang *et al*., 2025). After compressing the sample through a 0.05-mm sieve, the SOC components were determined by Fourier-transform infrared spectroscopy instrument (Nicolet IS 10, Thermo Fisher Scientific, USA) (Farnet-Da Silva *et al*., 2017). During scanning, air was used as the background, and 32 scans were conducted at a resolution of 4 cm^{-1} in the spectral range of 500–4 000 cm^{-1}. Different SOC components were represented by their functional groups. The functional groups and their main peak vibration ranges were as follows: polysaccharide C, 1 060–1 170 cm^{-1} (C–O); methyl C, 1 350–1 445 cm^{-1} (C–H); aromatic C, 1 600–1 660 cm^{-1} (C=C); carboxyl C, 1 710–1 720 cm^{-1} (C=O); and aliphatic C, 2 800–3 000 cm^{-1} (C–H). To enhance our understanding of SOC and the relationships between its composition and bacterial communities, we classified polysaccharide, methyl, and aliphatic C as labile SOC and aromatic and carboxyl C as recalcitrant SOC based on a previous study of Peltre *et al*. (2014).

A semi-quantitative analysis was conducted in the Omnic software by applying baseline correction, smoothing, and coordinate normalization to the infrared spectra. The spectral data were analyzed using Origin 2022 and peak analysis, and baseline selection and peak area integration were conducted based on the selected absorption peaks to determine the relative percentages of SOC components (Sun *et al*., 2019). The content of an SOC component was expressed as the product of the relative percentage of the SOC component and the SOC content.

DNA extraction, high-throughput sequencing, and data analysis

Soil DNA extraction, high-throughput sequencing, and sequencing data processing were conducted. The methods used and relevant references are presented in Appendix 1

(see Supplementary Material for Appendix 1). All data were stored in the National Center for Biotechnology Information (NCBI) Sequence Reading Archive (SRA) database under the accession number PRJNA1048133.

After obtaining the operational taxonomic unit (OTU) sequences, the classification of total taxa was realized by calculating the relative abundances of all OTUs. The OTU sequences with a relative abundance exceeding 0.1% of the total abundance were defined as abundant taxa, whereas those with a relative abundance below 0.01% were defined as rare taxa (Liu *et al*., 2015; Zheng *et al*., 2021). After taxonomic classification, Shannon index, Simpson index, ACE, and Chao 1 were calculated to represent the α-diversity of different taxa.

The "picante" package (Kembel *et al*., 2010) in R version 4.2.2 (R Core Team, 2016) was used to calculate the β-nearest taxon index (βNTI) for different bacterial taxa in OH and MH. Subsequently, based on the scripts in R obtained from previous studies (Chase and Myers, 2011; Stegen *et al*., 2013), the Bray-Curtis-based Raup-Crick index (RCBray) was calculated. These calculations helped determine the assembly mechanisms of bacterial communities for different taxa in OH and MH under P addition. Based on these results, the assembly of bacterial communities can be classified into stochastic and deterministic processes. Stochastic processes were characterized using $|\beta\text{NTI}| < 2$, with $|\text{RCBray}| < 0.95$ indicating an undominated process, $\text{RCBray} < -0.95$ indicating homogenizing dispersal, and $\text{RCBray} > 0.95$ indicating dispersal limitation. Conversely, deterministic processes were indicated using $\beta\text{NTI} < -2$ and $\beta\text{NTI} > 2$, representing homogeneous and heterogeneous selections, respectively (Tripathi *et al*., 2018; Zheng *et al*., 2021; Ye *et al*., 2023).

Statistical analysis

One-way analysis of variance was conducted using IBM SPSS Statistics 23. For data that did not meet the normal distribution assumption, the Kruskal-Wallis test was conducted at a significance level of $P < 0.05$, and Origin 2023b was used for visualization. The relationships between soil physicochemical properties, enzyme activities, and SOC components, as well as those between soil physicochemical properties, enzyme activities, and bacterial community characteristics, were analyzed using redundancy analysis (RDA) in CANOCO 5.0. The relationships between SOC components and bacterial community characteristics were visualized using the "corrplot" package in R, which was used to generate a pie-chart correlation heatmap.

Partial-least squares path modeling (PLS-PM) was applied to obtain more accurate model prediction results to further understand the influences of soil physicochemical properties and SOC composition on bacterial community characteristics and assembly processes in OH and MH. The goodness of fit (GOF) test was used to evaluate the models with different components.

RESULTS

Soil physicochemical properties and enzyme activity characteristics

Compared with CK, P addition resulted in increased soil TP and AP contents by 2.8%–13.6% in OH and 3.2%–16.4% in MH and 19.3%–38.9% in OH and 19.0%–23.8% in MH, respectively (Fig. S2, see Supplementary Material for Fig. S2). Under P addition, the activities of various enzymes significantly altered in different soil layers, with all treatments showing higher enzyme activities in OH than in MH (Table SI, see Supplementary Material for Table SI). In OH, the βG activity increased with P addition, reaching its highest level in the P4 treatment, 47.6% higher than that in CK. The CBH activity initially increased and subsequently decreased with P addition in both OH and MH, peaking in the P1 and P2 treatments in OH and MH, respectively.

Content and composition of SOC

Addition of P significantly influenced the SOC content and its composition (Table I). The SOC content in OH was consistently higher than that in MH across all treatments, with an excess range of 8.3%–44.1%. Additionally, the labile SOC fraction, including polysaccharide, methyl, and aliphatic C, was also higher in OH than in MH. Under P addition, the SOC content increased by 28.6%–44.1% in OH and 14.3%–39.4% in MH compared with that in CK. With increasing levels of P addition, both polysaccharide and methyl C in OH showed an upward trend, peaking in the P4 treatment. Conversely, the recalcitrant SOC fraction (aromatic and carboxylic C) increased initially, peaking in the P1 treatment, and then decreased. In MH, aromatic and carboxylic C gradually increased, reaching their maximum values in the P4 treatment (Table I, Fig. 1).

Correlations of SOC and its component with soil physicochemical properties and enzyme activities

The RDA results revealed significant differences in soil physicochemical properties, enzyme activities, and SOC and its composition between different soil layers in response to P addition (Fig. S3, see Supplementary Material for Fig. S3). In OH, the labile SOC fraction was positively correlated with βG, NAG, TP, AP, NO_3^--N, and NH_4^+-N, but negatively correlated with pH. Additionally, the recalcitrant SOC fraction was positively correlated with CBH and TN, but negatively correlated with ALP. In MH, the labile and recalcitrant SOC fractions, except for aliphatic C, were positively correlated with CBH, NO_3^--N, TN, ALP, and AP. The recalcitrant SOC fraction also showed a positive correlation with TP, whereas all five C components were negatively correlated with NAG, NH_4^+-N, and pH.

TABLE I

Contents and composition of soil organic C (SOC) in organic horizon (OH) and mineral horizon (MH) in the treatments with no P addition (control, CK) and with P addition at 0.5 (P1), 1 (P2), 2 (P3), and 4 (P4) g P m^{-2} $year^{-1}$ in an artificial *Robinia pseudoacacia* forest

Horizon	Treatment	SOC	Polysaccharide C	Methyl C	Aliphatic C	Aromatic C	Carboxylic C
		g kg^{-1}					
OH	CK	14.09 ± 0.81[a)]d[b)]	4.72 ± 0.50d	2.71 ± 0.13d	3.73 ± 0.26ab	2.46 ± 0.21e	0.48 ± 0.05c
	P1	21.04 ± 0.21b	7.01 ± 0.33bc	4.09 ± 0.44c	3.68 ± 0.27ab	5.57 ± 0.11a	0.71 ± 0.03a
	P2	19.73 ± 0.31c	6.97 ± 0.16c	6.81 ± 0.55ab	2.52 ± 0.16c	3.05 ± 0.21d	0.38 ± 0.02d
	P3	23.01 ± 0.93b	7.95 ± 0.52b	6.70 ± 0.43b	3.95 ± 0.22a	3.87 ± 0.30c	0.53 ± 0.06b
	P4	25.19 ± 0.22a	9.93 ± 0.31a	7.78 ± 0.03a	3.39 ± 0.25b	4.24 ± 0.14b	0.53 ± 0.01b
MH	CK	11.02 ± 0.21d	4.50 ± 0.13b	3.32 ± 0.04d	1.19 ± 0.03c	1.72 ± 0.03d	0.29 ± 0.05b
	P1	12.86 ± 0.60c	3.50 ± 0.34c	3.52 ± 0.22cd	3.35 ± 0.72b	2.24 ± 0.14cd	0.24 ± 0.01b
	P2	17.84 ± 0.25b	7.16 ± 0.28a	5.44 ± 0.19b	1.45 ± 0.15c	3.30 ± 0.28b	0.48 ± 0.05a
	P3	16.67 ± 0.29b	4.43 ± 0.26bc	4.11 ± 0.19c	5.06 ± 0.20a	2.71 ± 0.17bc	0.36 ± 0.02b
	P4	23.25 ± 0.51a	8.12 ± 0.46a	6.64 ± 0.22a	3.86 ± 0.86ab	4.05 ± 0.22a	0.58 ± 0.05a

[a)] Means ± standard errors ($n = 5$).
[b)] Means followed by different letters within each column for a given soil horizon are significantly different at $P < 0.05$.

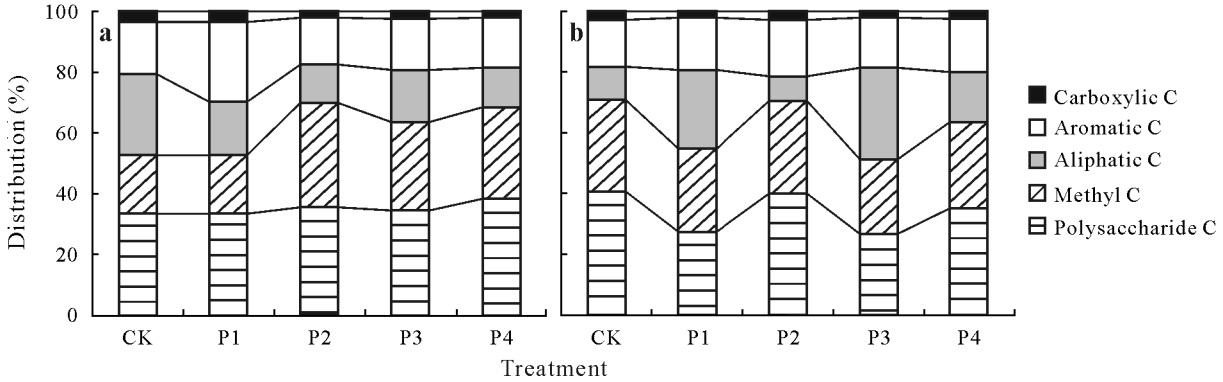

Fig. 1 Distributions of soil organic C (SOC) components in organic horizon (a) and mineral horizon (b) in the treatments with no P addition (control, CK) and with P addition at 0.5 (P1), 1 (P2), 2 (P3), and 4 (P4) g P m^{-2} $year^{-1}$ in an artificial *Robinia pseudoacacia* forest.

Soil bacterial community composition and diversity

Independent of P addition, the composition of soil bacterial community was dominated by Actinobacteria and Proteobacteria, which together accounted for 56.9%–62.0% of the total bacterial community (Fig. 2). With increasing P levels, a significant increase ($P < 0.05$) was observed in the proportions of Proteobacteria and Bacteroidetes in the OH, with increases of 20.1%–32.4% and 41.1%–53.0%, respectively, compared with those in CK. In MH, the proportions of Actinobacteria and Firmicutes increased ($P < 0.05$), reaching their peak values in the P4 treatment with increases of 17.9% and 51.4%, respectively, compared with CK. Although the dominant phyla were aligned with the bacterial community composition, changes in the composition of abundant and rare bacterial communities were not statistically significant ($P > 0.05$) with P addition.

The response of α-diversity of bacterial communities to P addition differed between OH and MH (Fig. S4, see Supplementary Material for Fig. S4). In OH, regardless of the total, abundant, or rare taxa, the response of bacterial diversity to P addition was not significant. However, in MH, bacterial community diversity was significantly affected ($P < 0.05$) by P addition. With increasing P levels, the Simpson index of both total and rare taxa significantly increased ($P < 0.05$), while the Simpson index of bacterial communities with abundant taxa decreased significantly ($P < 0.05$).

Assembly processes of different bacterial taxa

By analyzing phylogenetic trees and community abundance data, the effect of P addition on microbial community assembly was evaluated in OH and MH using the βNTI (Fig. 3). In general, both the total and rare bacterial taxa showed stochastic assembly processes across different soil layers. Abundant bacterial taxa also exhibited stochastic assembly, except in OH, where P addition caused a shift toward deterministic processes, with $|\beta NTI| > 2$ observed in the P4 treatment. Conversely, in MH, the assembly process transitioned from deterministic to stochastic as P addition increased, displaying an opposite pattern to that seen in OH.

The partitioning of assembly modes for abundant and rare bacterial communities across soil layers (Fig. 4) revealed that in OH, the abundant bacterial community predominantly assembled through dispersal limitation, shifting to

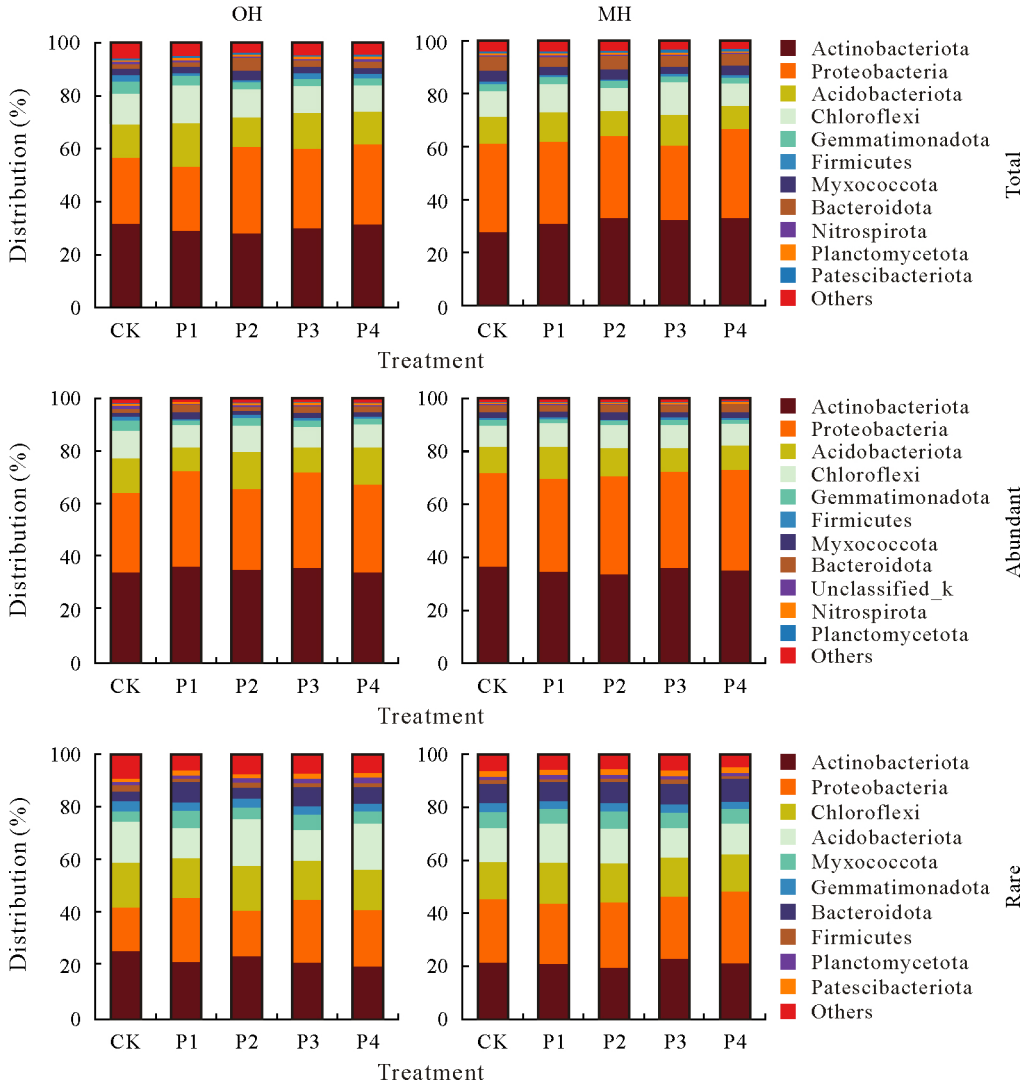

Fig. 2 Distributions of total, abundant, and rare bacterial taxa in soil organic horizon (OH) and mineral horizon (MH) in the treatments with no P addition (control, CK) and with P addition at 0.5 (P1), 1 (P2), 2 (P3), and 4 (P4) g P m^{-2} $year^{-1}$ in an artificial *Robinia pseudoacacia* forest.

heterogeneous selection with P addition. In contrast, in MH, the assembly mode shifted from heterogeneous selection to dispersal limitation. Considering the rare bacterial community, the primary modes of assembly across different soil layers were homogeneous dispersal and selection.

Correlations between bacterial community and SOC components

Pie-chart correlation heatmaps were constructed to explore the relationships between SOC components and bacterial community composition and diversity across different soil layers (Fig. 5). In OH, total, abundant, and rare bacterial communities were primarily influenced by the labile SOC fraction, with aliphatic C showing correlations with microbial community diversity and composition. In MH, the total, abundant, and rare bacterial communities were influenced by both labile and recalcitrant SOC fractions.

Correlations between soil properties, SOC components, and bacterial community assembly processes

Through PLS-PM, the effect of P addition on the assembly processes of different bacterial communities was elucidated, with SOC components serving as intermediaries between soil physicochemical properties (*e.g.*, AP), microbial community characteristics, and community assembly processes. The explained variance (R^2) for the assembly of various bacterial communities across different soil layers ranged from 0.42 to 0.81, and the GOF for the overall model was $\geqslant$ 0.60 (Fig. 6). Considering the total bacterial community in OH, AP directly regulated bacterial community assembly, with a standardized total effect of 1.18. In MH, the labile SOC fraction indirectly influenced bacterial community assembly by altering the bacterial community diversity, with a standardized total effect of 0.56.

The examination of various bacterial taxa revealed that

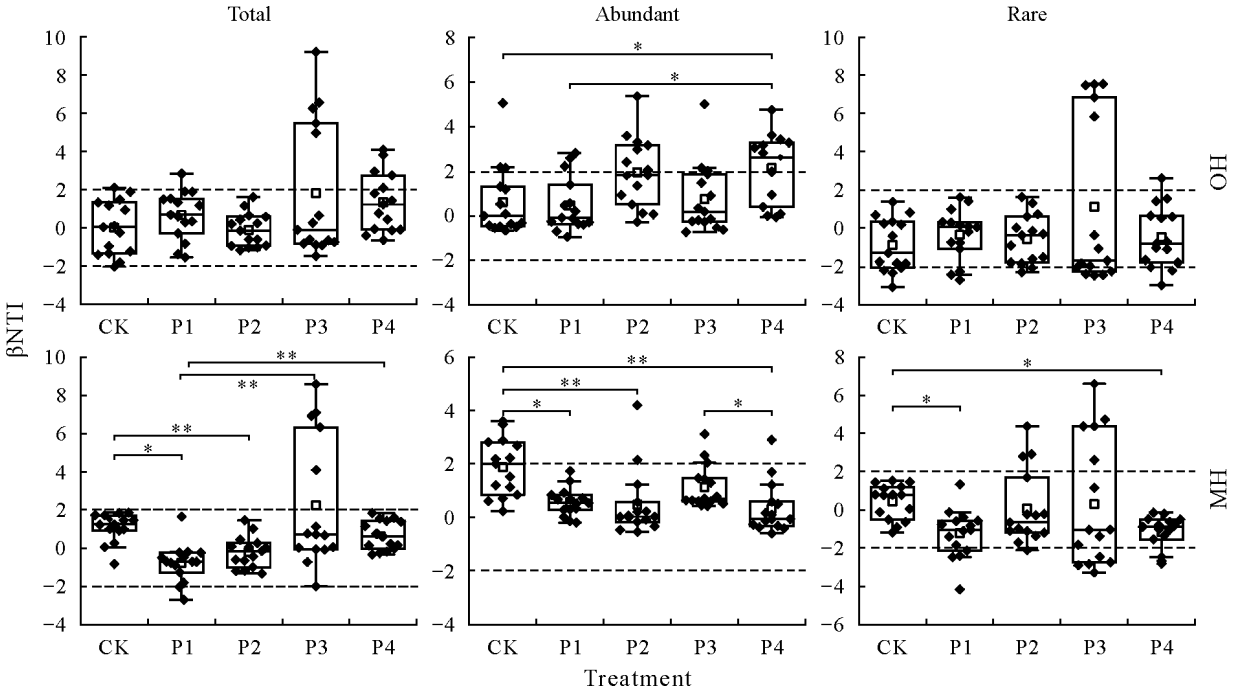

Fig. 3 Box plots of β-nearest taxon index (βNTI) of total, abundant, and rare bacterial taxa in soil organic horizon (OH) and mineral horizon (MH) in the treatments with no P addition (control, CK) and with P addition at 0.5 (P1), 1 (P2), 2 (P3), and 4 (P4) g P m^{-2} $year^{-1}$ in an artificial *Robinia pseudoacacia* forest. When $|\beta NTI| > 2$, bacterial community is considered a deterministic assembly, while when $|\beta NTI| < 2$, bacterial community is considered a stochastic assembly. The positions of -2 and 2 are marked with dashed lines. Asterisks * and ** indicate significant differences at $P < 0.05$ and $P < 0.01$, respectively, according to the Kruskal-Wallis test.

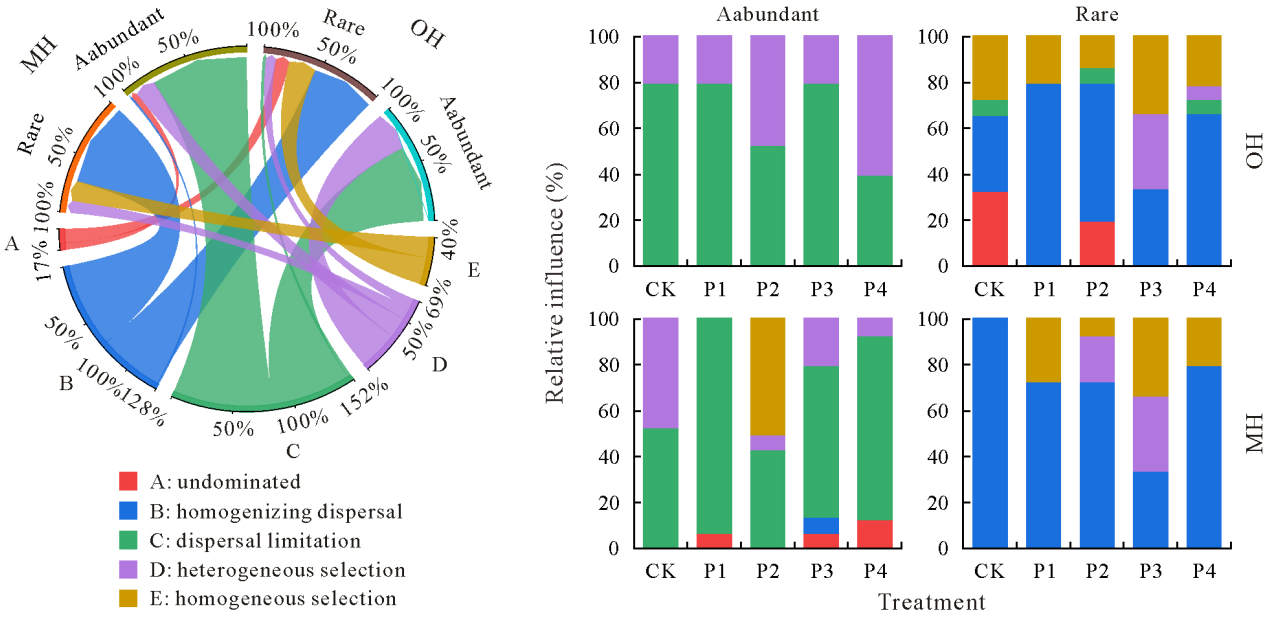

Fig. 4 Relative influences of deterministic and stochastic assembly processes in shaping abundant and rare bacterial communities in soil organic horizon (OH) and mineral horizon (MH) in the treatments with no P addition (control, CK) and with P addition at 0.5 (P1), 1 (P2), 2 (P3), and 4 (P4) g P m^{-2} $year^{-1}$ in an artificial *Robinia pseudoacacia* forest. Stochastic processes (see legends A, B, and C) are characterized using $|\beta NTI| < 2$, with $|RCBray| < 0.95$ indicating an undominated process, $RCBray < -0.95$ indicating homogenizing dispersal, and $RCBray > 0.95$ indicating dispersal limitation. Conversely, deterministic processes (see legends C and D) are indicated using $\beta NTI > 2$ and $\beta NTI < -2$, representing heterogeneous and homogeneous selections, respectively. βNTI = β-nearest taxon index; RCBray = Bray-Curtis-based Raup-Crick index.

the assembly of abundant bacterial taxa was influenced by the labile and recalcitrant SOC fractions in OH (standardized total effect = 0.82) and MH (standardized total effect = 0.62), respectively. In contrast to the abundant bacterial taxa, the assembly of rare bacterial taxa was regulated by the labile SOC fraction in both OH (standardized total effect = −1.12)

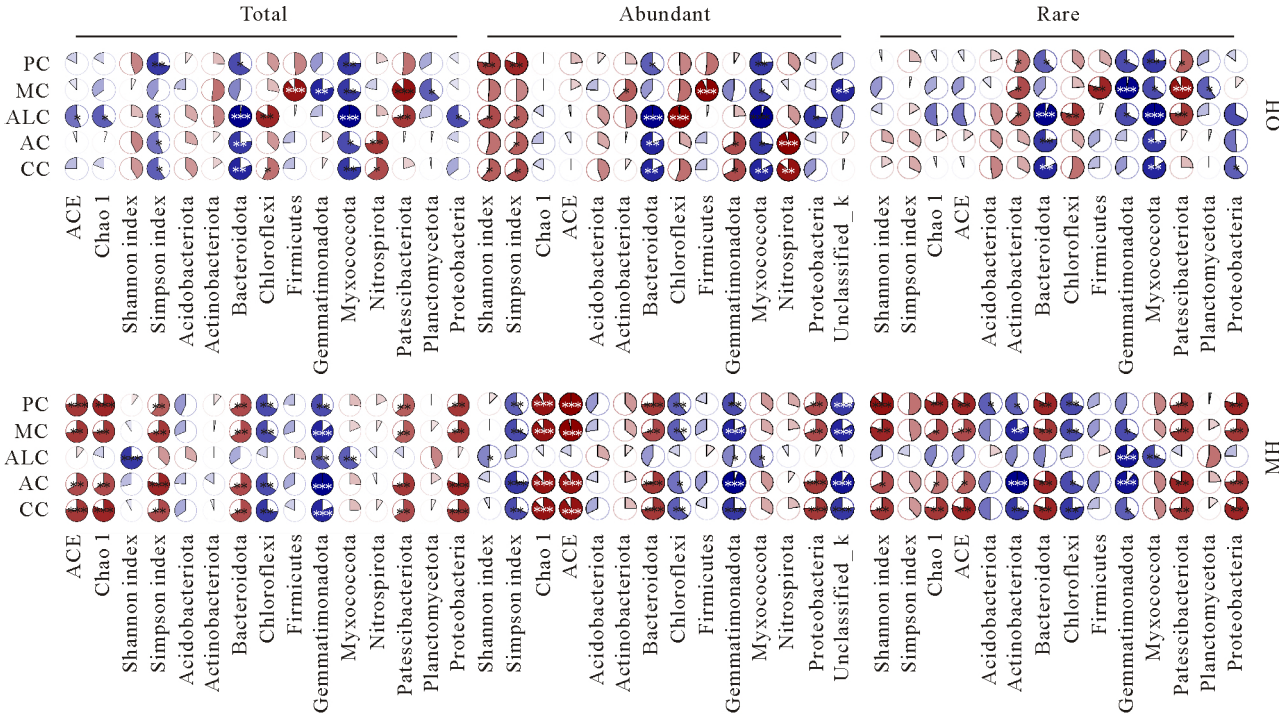

Fig. 5 Pie-chart correlation heatmaps showing the correlations between soil organic C components and the diversity and composition of total, abundant, and rare bacterial taxa in soil organic horizon (OH) and mineral horizon (MH) in the treatments with no P addition and with P addition at different levels in an artificial *Robinia pseudoacacia* forest. The fuller the pie chart and the deeper the color, the greater the correlation. PC = polysaccharide C; MC = methyl C; ALC = aliphatic C; AC = aromatic C; CC = carboxylic C. Asterisks *, **, and *** indicate significant correlations at $P < 0.05$, $P < 0.01$, and $P < 0.001$, respectively, according to the Kruskal-Wallis test.

and MH (standardized total effect = 0.85). These results indicate that under P addition, AP and SOC composition affected the bacterial community assembly processes.

DISCUSSION

Effects of P addition on SOC and its composition

Our results showed that P addition significantly increased the SOC content (Table I), consistent with the results of Feng *et al*. (2023). This is because P addition can promote the above- and belowground growth of plants, resulting in more litter, root residues, and C input from root exudates to the soil and then leading to an increase in SOC (Sun *et al*., 2022). Additionally, under P addition, the activities of some extracellular enzymes in soil increased (Table SI), accelerating the conversion of plant and microbial residues into SOC (Gong *et al*., 2023). The increase in SOC content in different soil layers promoted the production of organic acids in the soil, thereby reducing soil pH (Liu *et al*., 2020).

Addition of P also increased the contents of various SOC fractions (Table I). Specifically, the relative contents of polysaccharide and methyl C increased in OH, whereas aromatic and carboxyl C increased in MH (Fig. 1). This observation supports our first hypothesis. In OH, the explanation for this pattern is that P addition promotes plant growth, enhancing litter production (Hou *et al*., 2020; Xu *et al*., 2020; Shi *et al*., 2023) and augmenting the source of labile SOC fraction. Simultaneously, the recalcitrant SOC fraction in OH migrates into MH, reducing this fraction in OH and increasing this fraction in MH. The elevated presence of recalcitrant SOC fraction in MH can also be attributed to the promotion of root growth by P addition (Jiang *et al*., 2021), leading to an increase in root exudates and root residues. Furthermore, P addition to OH increases the number of free P ions that are adsorbed onto mineral surfaces (Kleber *et al*., 2015; Ma *et al*., 2023), inhibiting the binding of microbial residues with minerals and impeding the formation of recalcitrant SOC fraction. However, in MH, where the mineral content surpasses that in OH, microbial residues can readily combine with minerals to form a recalcitrant SOC fraction (Li *et al*., 2021).

Effects of P addition on soil bacterial community composition and diversity

Under P addition, the bacterial community composition in the different soil layers was dominated by Actinobacteria and Proteobacteria (Figs. 2 and S5, see Supplementary Material for Fig. S5). This dominance was attributed to their robust adaptability and competitive advantage over other bacterial phyla in terms of nutrient resources (Dai *et al*., 2018). Consequently, they thrive in the loose and poor soils

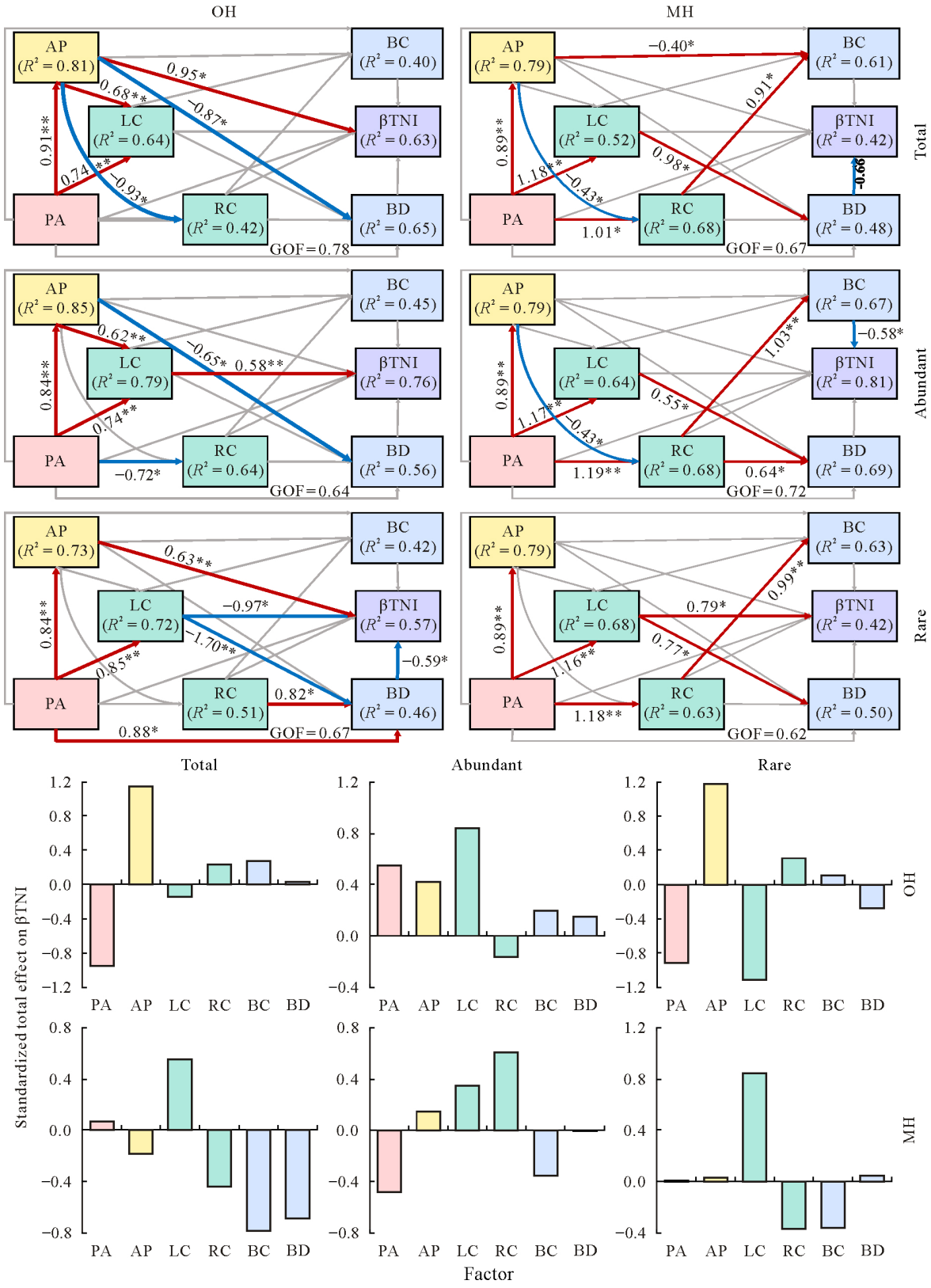

Fig. 6 Partial least squares path modeling and standardized total effects quantifying the direct or indirect effects of soil properties and soil organic C (SOC) components on community structure characteristics and assembly processes of total, abundant, and rare bacterial taxa in soil organic horizon (OH) and mineral horizon (MH) under P addition (PA) in an artificial *Robinia pseudoacacia* forest. The red and blue lines with path coefficients indicate positive and negative correlations, respectively. Labile SOC (LC), recalcitrant SOC (RC), bacterial composition (BC), and bacterial diversity (BD) were the first axes of the principal component analysis based on polysaccharide, methyl, and aliphatic C, aromatic and carboxylic C, the abundances of the top 8 phyla, and Simpson index and ACE, respectively. Asterisks * and ** indicate significances at $P < 0.05$ and $P < 0.01$, respectively, according to the Kruskal-Wallis test. AP = available P; βNTI = β-nearest taxon index.

of the Loess Plateau, establishing themselves as the predominant phyla in the artificial forest ecosystems of this study region (Xu *et al*., 2020; Zhong *et al*., 2020). However, with increasing P levels, the proportions of Proteobacteria and Bacteroidetes increased in OH and decreased in MH, whereas those of Actinobacteria and Firmicutes exhibited the opposite trend (Fig. 2). This is because Proteobacteria and Bacteroidetes are Gram-negative bacteria that prefer environments with ample nutrient conditions and exhibit strong competitiveness (Yang *et al*., 2023). Consequently, under P addition, the increased nutrient resources in OH (Fig. S2) were preferentially utilized by Proteobacteria and Bacteroidetes. Conversely, Actinobacteria and Firmicutes, classified as Gram-positive bacteria, demonstrate robust adaptability and can thrive in the relatively nutrient-poor MH (Yang *et al*., 2023). This variation is contingent on the disparity in SOC composition between OH and MH under P addition. Addition of P increased the labile SOC fraction in OH (Fig. 1), creating an environment rich in labile SOC that is favored by r-strategist species, such as Proteobacteria and Bacteroidetes, which have low substrate affinity (Delgado-Baquerizo *et al*., 2016). In contrast, the recalcitrant SOC fraction in MH increased with P addition (Fig. 1), providing an optimal growth habitat for K-strategist species, such as Actinobacteria and Firmicutes, which grow slowly, possess high substrate affinity, and can effectively utilize the recalcitrant SOC fraction (Ling *et al*., 2021; Shi *et al*., 2023). Furthermore, the results of RDA (Fig. S6, see Supplementary Material for Fig. S6) indicated that in OH, AP had the greatest contribution to the changes in bacterial community. This is because the availability of P provides the necessary nutrient conditions for the composition of oligotrophic and copiotrophic bacteria in OH (Zhou *et al*., 2024). Considering bacterial taxa, the effect of P addition on the composition of abundant and rare bacterial communities in both OH and MH was not significant (Fig. 2). This is attributed to the inherent stability and resistance to environmental disturbances caused by abundant and rare bacterial taxa, respectively (Ye *et al*., 2023), which led to their adaptation to the barren soil of the Loess Plateau. Therefore, P addition did not cause significant changes in community composition. Additionally, the non-significant effects may also be attributed to the concentration of added P (0–4 g P m^{-2} $year^{-1}$) in this study, which may not have exerted a notable influence on the composition of abundant and rare bacterial taxa. For example, Li *et al*. (2021) and Wang *et al*. (2023) showed that when P was added at a concentration of 8–10 g P m^{-2} $year^{-1}$, the composition of abundant and rare bacterial communities was significantly altered.

Moreover, P addition had differing effects on the α-diversity of bacterial communities in OH and MH. In OH, P addition did not significantly influence the bacterial community diversity, whereas in MH, community diversity showed an increasing trend (Fig. S4). This may be attributed to the enrichment of labile SOC fraction in OH owing to P addition, resulting in reduced competition among bacterial communities (Jiao *et al*., 2022). The enhanced effectiveness of P supported the majority of bacterial activity (Fig. S6), thereby sustaining the stability of bacterial community diversity in OH (Huang *et al*., 2021; Teste *et al*., 2021). However, in MH, the levels of labile SOC and effective nutrients were lower than those in OH (Figs. 1 and S2), which intensifies the competition among bacterial communities for resources and stimulates greater species diversification (Bailey *et al*., 2013; Wu *et al*., 2023), leading to an increase in bacterial diversity in MH (Fig. S4). From the perspective of bacterial taxa, following P addition, the diversity of both abundant and rare bacterial communities in OH remained unchanged, similar to that of the total bacterial community. In MH, the diversities of abundant and rare taxa decreased and increased, respectively (Fig. S4). Considering abundant bacterial taxa in MH, the AP content increased with P addition, providing a favorable environment for abundant bacteria (Jiao and Lu, 2020). However, the proportion of recalcitrant SOC fraction in MH increased, leading to the rapid occupation of more ecological niches by bacteria that prefer recalcitrant SOC fraction (Fig. 5). Consequently, the growth and development of abundant bacterial taxa sensitive to labile SOC fraction (Liu *et al*., 2020) are restricted, thereby reducing bacterial community diversity. Additionally, compared with those in CK, SOC resources in MH increased under P addition, which intensified the competition for resources and niches among rare taxa of bacterial species (Zhang *et al*., 2022) that occupy relatively narrow ecological niches (Jousset *et al*., 2017), thereby promoting the diversity of rare bacterial communities. Simultaneously, the increase in the diversity of rare bacteria in MH substantiates the dominance of rare bacteria in driving the total bacterial community diversity.

Effect of P addition on assembly processes of soil bacterial communities

Stochastic processes dominated the assembly of bacterial community in the soil of RP forest under P addition (Fig. 3). This is attributed to the increase in P, which augmented soil nutrient resources (Fig. S2). Consequently, this facilitates the turnover and propagation of bacterial communities, leading to stochastic birth, drift, and dispersion within bacterial community. Ultimately, these stochastic assembly processes become more pronounced with P addition (Ning *et al*., 2020). However, regulatory factors for bacterial community assembly varied in different soil layers. In OH, the assembly processes were directly regulated by AP (Fig. 6). This is attributed to the increase in AP caused by P addition, which reduces environmental filtering and intra-community niche exclusion owing to the scarcity of available nutrient resources

during community assembly (Jiao and Lu, 2020; Chen and Xiao, 2023). Consequently, the bacterial communities in OH assembled stochastically. This observation aligns with that of Tripathi *et al*. (2018), who suggested that bacterial communities tend to aggregate stochastically in neutral environments from an evolutionary perspective. However, in MH, the assembly processes were primarily influenced by labile SOC fraction (Fig. 6). This is because MH has lower effective nutrient levels than OH, leading to increased environmental pressure. However, the labile SOC content increased with P addition (Table I), augmenting the supply of effective substrates to MH (Zhu *et al*., 2023). This stimulates niche differentiation among bacterial communities, reducing the environmental filtering effects that the bacterial communities in MH may experience owing to lower effective resource levels (Huang *et al*., 2021; Shi *et al*., 2023). Consequently, the bacterial communities in MH became more diverse and underwent stochastic assembly processes.

Although P addition promoted the assembly of bacterial communities dominated by stochastic processes, the assembly processes of abundant taxa in the bacterial communities exhibited different patterns in OH and MH. With increasing levels of P addition, the assembly processes of abundant bacterial taxa transitioned from stochastic to deterministic processes in OH and from deterministic to stochastic processes in MH (Fig. 3), supporting our second hypothesis. With increasing levels of P addition, the turnover and decomposition of litter in OH accelerate, enhancing environmental heterogeneity (Luan *et al*., 2020). This results in abundant bacterial taxa in OH that experience greater environmental filtering, thereby strengthening the deterministic assembly of bacterial communities (Ye *et al*., 2023). Additionally, the assembly of abundant bacterial taxa in OH was influenced by labile SOC fraction (Fig. 6). This is attributed to the increase in labile SOC in OH that has a fast turnover rate. Consequently, there is an increase in copiotrophic bacteria with high substrate affinity among the abundant taxa, reducing the competitive ability of oligotrophic bacteria (Yang *et al*., 2023). Consequently, the abundant taxa experience competitive pressure within the community (Wu *et al*., 2023). Moreover, in OH, the faster nutrient turnover enhances the heterogeneous selection process in the environment (Fig. 4), leading to a shift from stochastic to deterministic assembly processes for abundant taxa in OH (Zhou and Ning, 2017). In contrast, the environmental heterogeneity in MH was lower than that in OH (Crumsey *et al*., 2015), providing a favorable medium for the movement and dispersal of abundant taxa. Additionally, compared with those in CK, the SOC resources in MH increased with P addition, facilitating the movement and dispersion of abundant taxa under conditions of weak environmental selection (Chen *et al*., 2023). However, the increase of recalcitrant SOC content in MH limited the diffusion of bacterial composition with high substrate affinity among abundant taxa (Fig. 6). Therefore, the transition in the assembly of abundant taxa in MH was mainly dominated by dispersal limitation (Fig. 4).

In contrast to the assembly of abundant bacterial taxa, that of rare bacterial taxa in both OH and MH exhibited stochastic processes (Fig. 3). This is because rare bacterial taxa have small individual volumes but large community abundances, are widely distributed in OH and MH (Zheng *et al*., 2021), and can freely disperse between layers. This high dispersal rate leads to the homogenization of the structure of rare taxa in bacterial communities (Wu *et al*., 2023). The phylogenetic direction was more dispersed, suggesting that rare taxa in the bacterial communities were stochastically assembled under the dominance of homogeneous dispersal (Fig. 4). Additionally, according to the results of the PLS-PM and total effect models, the primary factor driving the assembly of rare taxa in OH and MH was labile SOC fraction (Fig. 6). This was because P addition increased the labile SOC content in OH and MH (Table I), providing energy for the stochastic occurrence and dispersal of rare bacteria in OH and MH. This facilitates the free dispersion of rare bacteria in narrow ecological niches (Ji *et al*., 2020) and regulates the diversity of rare bacterial communities in OH and MH, thereby influencing their assembly (Wan *et al*., 2021; Zhang *et al*., 2022). However, community structure does not undergo turnover owing to the strong environmental resistance of rare taxa (Peng *et al*., 2021; Cao *et al*., 2023). This followed stochastic processes dominated by homogeneous dispersal.

CONCLUSIONS

The addition of P altered soil physicochemical properties, particularly AP and SOC contents in both OH and MH, subsequently driving changes in the composition of bacterial communities. Under P addition, the assembly of total and rare bacterial taxa occurred through stochastic processes in both OH and MH. However, in OH, the assembly of abundant bacterial taxa shifted from stochastic to deterministic processes, whereas in MH, it shifted in the opposite direction. Key factors influencing the assembly of bacterial communities during P addition were AP and SOC, wherein SOC component played a crucial role in shaping bacterial taxa. These findings improve our understanding of bacterial community assembly in different soil layers under P addition in artificial forests, providing insights into the dynamic changes in bacterial communities induced by P addition.

DECLARATION OF COMPETING INTEREST

The authors declare that they have no known competing financial interests or personal relationships that could have appeared to influence the work reported in this paper.

ACKNOWLEDGEMENT

This work was supported by the Research and Demon-

stration of Collaborative Improvement Technology for Ecological Production Efficiency of Degraded Grasslands in Sandy Areas of Yulin City, China (No. 2023-CXY-180), the Shaanxi Forestry Science and Technology Innovation Plan, China (No. SXLK2022-02-14), the Chinese Universities Scientific Fund (No. 2452023079), and the National Forage Industry Technology System Program of China (No. CARS-34).

SUPPLEMENTARY MATERIAL

Supplementary material for this article can be found in the online version.

REFERENCES

Bailey S F, Dettman J R, Rainey P B, Kassen R. 2013. Competition both drives and impedes diversification in a model adaptive radiation. *Proc Roy Soc B Biol Sci*. **280**: 20131253.

Cao H, Li S Y, He H, Sun Y Q, Wu Y C, Huang Q Y, Cai P, Gao C H. 2023. Stronger linkage of diversity-carbon decomposition for rare rather than abundant bacteria in woodland soils. *Front Microbiol*. **14**: 1115300.

Chase J M. 2010. Stochastic community assembly causes higher biodiversity in more productive environments. *Science*. **328**: 1388–1391.

Chase J M, Myers J A. 2011. Disentangling the importance of ecological niches from stochastic processes across scales. *Philos Trans Roy Soc B Biol Sci*. **366**: 2351–2363.

Chen C, Xiao W Y. 2023. The global positive effect of phosphorus addition on soil microbial biomass. *Soil Biol Biochem*. **176**: 108882.

Chen X D, Li H, Condron L M, Dunfield K E, Wakelin S A, Mitter E K, Jiang N. 2023. Long-term afforestation enhances stochastic processes of bacterial community assembly in a temperate grassland. *Geoderma*. **430**: 116317.

Crumsey J M, Capowiez Y, Goodsitt M M, Larson S, Le Moine J M, Bird J A, Kling G W, Nadelhoffer K J. 2015. Exotic earthworm community composition interacts with soil texture to affect redistribution and retention of litter-derived C and N in northern temperate forest soils. *Biogeochemistry*. **126**: 379–395.

Dai Z M, Su W Q, Chen H H, Barberán A, Zhao H C, Yu M J, Yu L, Brookes P C, Schadt C W, Chang S X, Xu J M. 2018. Long-term nitrogen fertilization decreases bacterial diversity and favors the growth of *Actinobacteria* and *Proteobacteria* in agro-ecosystems across the globe. *Glob Change Biol*. **24**: 3452–3461.

Delgado-Baquerizo M, Maestre F T, Reich P B, Trivedi P, Osanai Y, Liu Y R, Hamonts K, Jeffries T C, Singh B K. 2016. Carbon content and climate variability drive global soil bacterial diversity patterns. *Ecolo Monogr*. **86**: 373–390.

Deng Q, Cheng X L, Hui D F, Zhang Q, Li M, Zhang Q F. 2016. Soil microbial community and its interaction with soil carbon and nitrogen dynamics following afforestation in central China. *Sci Total Environ*. **541**: 230–237.

Farnet-Da Silva A M, Ferré E, Dupuy N, de la Boussinière A, Rébufa C. 2017. Infra-red spectroscopy reveals chemical interactions driving water availability for enzyme activities in litters of typical Mediterranean tree species. *Soil Biol Biochem*. **114**: 72–81.

Feng J G, Song Y J, Zhu B. 2023. Ecosystem-dependent responses of soil carbon storage to phosphorus enrichment. *New Phytol*. **238**: 2363–2374.

Fontaine S, Barot S, Barré P, Bdioui N, Mary B, Rumpel C. 2007. Stability of organic carbon in deep soil layers controlled by fresh carbon supply. *Nature*. **450**: 277–280.

Gong J R, Dong X D, Li X B, Yue K X, Shi J Y, Song L Y, Zhang Z H, Zhang W Y, Li Y. 2023. Phosphorus fertilization affects litter quality and enzyme activity in a semiarid grassland. *Plant Soil*. **492**: 91–108.

Hao H J, Liang Y J, Pian D, Zhang Y, Chen Y X, Lai H T, Yu Z C, Sailike A, Wang R, Cao L, Han X H, Zhang W. 2024. Macroaggregate is crucial in soil carbon and nitrogen accumulation under different vegetation types in the Loess Plateau, China. *For Ecol Manage*. **569**: 122161.

Hou E Q, Luo Y Q, Kuang Y W, Chen C R, Lu X K, Jiang L F, Luo X Z, Wen D Z. 2020. Global meta-analysis shows pervasive phosphorus limitation of aboveground plant production in natural terrestrial ecosystems. *Nat Commun*. **11**: 637.

Huang Y L, Dai Z M, Lin J H, Li D M, Ye H C, Dahlgren R A, Xu J M. 2021. Labile carbon facilitated phosphorus solubilization as regulated by bacterial and fungal communities in *Zea mays*. *Soil Biol Biochem*. **163**: 108465.

Huang Y X, Wu Z J, Zong Y Y, Li W Q, Chen F S, Wang G G, Li J J, Fang X M. 2022. Mixing with coniferous tree species alleviates rhizosphere soil phosphorus limitation of broad-leaved trees in subtropical plantations. *Soil Biol Biochem*. **175**: 108853.

Ji M K, Kong W D, Stegen J, Yue L Y, Wang F, Dong X B, Cowan D A, Ferrari B C. 2020. Distinct assembly mechanisms underlie similar biogeographical patterns of rare and abundant bacteria in Tibetan Plateau grassland soils. *Environ Microbiol*. **22**: 2261–2272.

Jiang J, Wang Y P, Liu F C, Du Y, Zhuang W, Chang Z B, Yu M X, Yan J H. 2021. Antagonistic and additive interactions dominate the responses of belowground carbon-cycling processes to nitrogen and phosphorus additions. *Soil Biol Biochem*. **156**: 108216.

Jiao S, Chu H Y, Zhang B G, Wei X R, Chen W M, Wei G H. 2022. Linking soil fungi to bacterial community assembly in arid ecosystems. *iMeta*. **1**: e2.

Jiao S, Lu Y H. 2020. Soil pH and temperature regulate assembly processes of abundant and rare bacterial communities in agricultural ecosystems. *Environ Microbiol*. **22**: 1052–1065.

Jones D L, Willett V B. 2006. Experimental evaluation of methods to quantify dissolved organic nitrogen (DON) and dissolved organic carbon (DOC) in soil. *Soil Biol Biochem*. **38**: 991–999.

Jousset A, Bienhold C, Chatzinotas A, Gallien L, Gobet A, Kurm V, Küsel K, Rillig M C, Rivett D W, Salles J F, van der Heijden M G A, Youssef N H, Zhang X W, Wei Z, Hol W H G. 2017. Where less may be more: How the rare biosphere pulls ecosystems strings. *ISME J*. **11**: 853–862.

Kembel S W, Cowan P D, Helmus M R, Cornwell W K, Morlon H, Ackerly D D, Blomberg S P, Webb C O. 2010. Picante: R tools for integrating phylogenies and ecology. *Bioinformatics*. **26**: 1463–1464.

Kennedy A C. 1999. Bacterial diversity in agroecosystems. *Agr Ecosyst Environ*. **74**: 65–76.

Khan K S, Mack R, Castillo X, Kaiser M, Joergensen R G. 2016. Microbial biomass, fungal and bacterial residues, and their relationships to the soil organic matter C/N/P/S ratios. *Geoderma*. **271**: 115–123.

Kleber M, Eusterhues K, Keiluweit M, Mikutta C, Mikutta R, Nico P S. 2015. Mineral-organic associations: Formation, properties, and relevance in soil environments. *Adv Agron*. **130**: 1–140.

Li J H, Cheng B H, Zhang R, Li W J, Shi X M, Han Y W, Ye L F, Ostle N J, Bardgett R D. 2021. Nitrogen and phosphorus additions accelerate decomposition of slow carbon pool and lower total soil organic carbon pool in alpine meadows. *Land Degrad Dev*. **32**: 1761–1772.

Liang Y J, Fu R, Sailike A, Hao H J, Yu Z C, Wang R, Peng N, Li S C, Zhang W, Liu Y Y. 2025. Soil labile organic carbon and nitrate nitrogen are the main factors driving carbon-fixing pathways during vegetation restoration in the Loess Plateau, China. *Agr Ecosyst Environ*. **378**: 109283.

Ling L, Fu Y Y, Jeewani P H, Tang C X, Pan S T, Reid B J, Gunina A, Li Y F, Li Y C, Cai Y J, Kuzyakov Y, Li Y, Su W Q, Singh B P, Luo Y, Xu J M. 2021. Organic matter chemistry and bacterial community structure regulate decomposition processes in post-fire forest soils. *Soil Biol Biochem*. **160**: 108311.

Liu L M, Yang J, Yu Z, Wilkinson D M. 2015. The biogeography of abundant and rare bacterioplankton in the lakes and reservoirs of China. *ISME J*. **9**: 2068–2077.

Liu T, Wu X H, Li H W, Alharbi H, Wang J, Dang P, Chen X Y, Kuzyakov Y, Yan W D. 2020. Soil organic matter, nitrogen and pH driven change

in bacterial community following forest conversion. *For Ecol Manage*. **477**: 118473.

Luan L, Liang C, Chen L J, Wang H T, Xu Q S, Jiang Y J, Sun B. 2020. Coupling bacterial community assembly to microbial metabolism across soil profiles. *mSystems*. **5**: e00298-20.

Luo R Y, Kuzyakov Y, Liu D Y, Fan J L, Luo J F, Lindsey S, He J S, Ding W X. 2020. Nutrient addition reduces carbon sequestration in a Tibetan grassland soil: Disentangling microbial and physical controls. *Soil Biol Biochem*. **144**: 107764.

Luo R Y, Kuzyakov Y, Zhu B, Qiang W, Zhang Y, Pang X Y. 2022. Phosphorus addition decreases plant lignin but increases microbial necromass contribution to soil organic carbon in a subalpine forest. *Glob Change Biol*. **28**: 4194–4210.

Ma T, Yang Z Y, Shi B W, Gao W J, Li Y F, Zhu J X, He J S. 2023. Phosphorus supply suppressed microbial necromass but stimulated plant lignin phenols accumulation in soils of alpine grassland on the Tibetan Plateau. *Geoderma*. **431**: 116376.

Ning D L, Yuan M T, Wu L W, Zhang Y, Guo X, Zhou X S, Yang Y F, Arkin A P, Firestone M K, Zhou J Z. 2020. A quantitative framework reveals ecological drivers of grassland microbial community assembly in response to warming. *Nat Commun*. **11**: 4717.

Paz-Ferreiro J, Gascó G, Gutiérrez B, Méndez A. 2012. Soil biochemical activities and the geometric mean of enzyme activities after application of sewage sludge and sewage sludge biochar to soil. *Biol Fert Soils*. **48**: 511–517.

Peltre C, Bruun S, Du C W, Thomsen I K, Jensen L S. 2014. Assessing soil constituents and labile soil organic carbon by mid-infrared photoacoustic spectroscopy. *Soil Biol Biochem*. **77**: 41–50.

Peng Z H, Wang Z F, Liu Y, Yang T Y, Chen W M, Wei G H, Jiao S. 2021. Soil phosphorus determines the distinct assembly strategies for abundant and rare bacterial communities during successional reforestation. *Soil Ecol Lett*. **3**: 342–355.

Peñuelas J, Janssens I A, Ciais P, Obersteiner M, Sardans J. 2020. Anthropogenic global shifts in biospheric N and P concentrations and ratios and their impacts on biodiversity, ecosystem productivity, food security, and human health. *Glob Change Biol*. **26**: 1962–1985.

Peñuelas J, Poulter B, Sardans J, Ciais P, van der Velde M, Bopp L, Boucher O, Godderis Y, Hinsinger P, Llusia J, Nardin E, Vicca S, Obersteiner M, Janssens I A. 2013. Human-induced nitrogen-phosphorus imbalances alter natural and managed ecosystems across the globe. *Nat Commun*. **4**: 2934.

Qin J, Liu H M, Zhao J N, Wang H, Zhang H F, Yang D L, Zhang N Q. 2020. The roles of bacteria in soil organic carbon accumulation under nitrogen deposition in *Stipa baicalensis* steppe. *Microorganisms*. **8**: 326.

R Core Team. 2016. R: A Language and Environment for Statistical Computing. R Foundation for Statistical Computing, Vienna.

Shi J W, Yang L, Liao Y, Li J W, Jiao S, Shangguan Z P, Deng L. 2023. Soil labile organic carbon fractions mediate microbial community assembly processes during long-term vegetation succession in a semiarid region. *iMeta*. **2**: e142.

Shi Y, Dang K K, Dong Y H, Feng M M, Wang B R, Li J G, Chu H Y. 2020. Soil fungal community assembly processes under long-term fertilization. *Eur J Soil Sci*. **71**: 716–726.

Stegen J C, Lin X J, Fredrickson J K, Chen X Y, Kennedy D W, Murray C J, Rockhold M L, Konopka A. 2013. Quantifying community assembly processes and identifying features that impose them. *ISME J*. **7**: 2069–2079.

Su B Q, Shangguan Z P. 2021. Response of water use efficiency and plant-soil C:N:P stoichiometry to stand quality in *Robinia pseudoacacia* on the Loess Plateau of China. *Catena*. **206**: 105571.

Sun S Q, Wu Y H, Zhang J, Wang G X, DeLuca T H, Zhu W Z, Li A D, Duan M, He L. 2019. Soil warming and nitrogen deposition alter soil respiration, microbial community structure and organic carbon composition in a coniferous forest on eastern Tibetan Plateau. *Geoderma*. **353**: 283–292.

Sun Y, Wang C T, Chen X L, Liu S R, Lu X J, Chen H Y H, Ruan H H. 2022. Phosphorus additions imbalance terrestrial ecosystem C:N:P stoichiometry. *Glob Change Biol*. **28**: 7353–7365.

Teste F P, Lambers H, Enowashu E E, Laliberté E, Marhan S, Kandeler E. 2021. Soil microbial communities are driven by the declining availability of cations and phosphorus during ecosystem retrogression. *Soil Biol Biochem*. **163**: 108430.

Tripathi B M, Stegen J C, Kim M, Dong K, Adams J M, Lee Y K. 2018. Soil pH mediates the balance between stochastic and deterministic assembly of bacteria. *ISME J*. **12**: 1072–1083.

Wan W J, Liu S, Li X, Xing Y H, Chen W L, Huang Q Y. 2021. Bridging rare and abundant bacteria with ecosystem multifunctionality in salinized agricultural soils: From community diversity to environmental adaptation. *mSystems*. **6**: e01221-20.

Wang H, Liu S R, Schindlbacher A, Wang J X, Yang Y J, Song Z C, You Y M, Shi Z M, Li Z Y, Chen L, Ming A G, Lu L H, Cai D X. 2019. Experimental warming reduced topsoil carbon content and increased soil bacterial diversity in a subtropical planted forest. *Soil Biol Biochem*. **133**: 155–164.

Wang H Y, Nie Y, Butterly C R, Wang L, Chen Q H, Tian W, Song B B, Xi Y G, Wang Y. 2017. Fertilization alters microbial community composition and functional patterns by changing the chemical nature of soil organic carbon: A field study in a Halosol. *Geoderma*. **292**: 17–24.

Wang K K, Ren T, Yan J Y, Lu Z F, Cong R H, Li X K, Lu J W. 2023. Soil phosphorus availability alters the effects of straw carbon on microbial mediated phosphorus conversion. *Plant Soil*. **491**: 575–590.

Wu C X, Yan B S, Wei F R, Wang H L, Gao L Q, Ma H Z, Liu Q, Liu Y, Liu G B, Wang G L. 2023. Long-term application of nitrogen and phosphorus fertilizers changes the process of community construction by affecting keystone species of crop rhizosphere microorganisms. *Sci Total Environ*. **897**.

Xu M P, Li W J, Wang J Y, Zhu Y F, Feng Y Z, Yang G H, Zhang W, Han X H. 2022. Soil ecoenzymatic stoichiometry reveals microbial phosphorus limitation after vegetation restoration on the Loess Plateau, China. *Sci Total Environ*. **815**: 152918.

Xu M P, Lu XQ, Xu Y D, Zhong Z K, Zhang W, Ren C J, Han X H, Yang G H, Feng Y Z. 2020. Dynamics of bacterial community in litter and soil along a chronosequence of *Robinia pseudoacacia* plantations. *Sci Total Environ*. **703**: 135613.

Yan Y, Klinkhamer P G L, van Veen J A, Kuramae E E. 2019. Environmental filtering: A case of bacterial community assembly in soil. *Soil Biol Biochem*. **136**: 107531.

Yang Y, Dou Y X, Wang B R, Xue Z J, Wang Y Q, An S S, Chang S X. 2023. Deciphering factors driving soil microbial life-history strategies in restored grasslands. *iMeta*. **2**: e66.

Ye F, Sun Z H, Moore S S, Wu J P, Hong Y G, Wang Y. 2023. Discrepant effects of flooding on assembly processes of abundant and rare communities in riparian soils. *Microb Ecol*. **86**: 1164–1175.

Yu Y J, Wu M, Petropoulos E, Zhang J W, Nie J, Liao Y L, Li Z P, Lin X G, Feng Y Z. 2019. Responses of paddy soil bacterial community assembly to different long-term fertilizations in southeast China. *Sci Total Environ*. **656**: 625–633.

Yu Z C, Zhang W, Zhang L Y, Ma S H, Sun L, Liu Y S, Zhang Y, Ahejiang S, Shi J Y, Cao L, Zhou R L, Xie Z G, Li Z Y, Yang P Z. 2023. Efficient vegetation restoration in Mu Us Desert reduces microbial diversity due to the transformation of nutrient requirements. *Ecol Indic*. **154**: 110758.

Yue K, Fornara D A, Yang W Q, Peng Y, Peng C H, Liu Z L, Wu F Z. 2017. Influence of multiple global change drivers on terrestrial carbon storage: Additive effects are common. *Ecol Lett*. **20**: 663–672.

Zhang G Q, Zhang P, Cao Y. 2018. Ecosystem carbon and nitrogen storage following farmland afforestation with black locust (*Robinia pseudoacacia*) on the Loess Plateau, China. *J Forest Res*. **29**: 761–771.

Zhang Q, Wang X, Zhang Z J, Liu H Y, Liu Y Y, Feng Y Z, Yang G H, Ren C J, Han X H. 2022. Linking soil bacterial community assembly with the composition of organic carbon during forest succession. *Soil Biol Biochem*. **173**: 108790.

Zhang W, Xu Y D, Gao D X, Wang X, Liu W C, Deng J, Han X H, Yang G H, Feng Y Z, Ren G X. 2019. Ecoenzymatic stoichiometry and nutrient dynamics along a revegetation chronosequence in the soils of abandoned land and *Robinia pseudoacacia* plantation on the Loess Plateau, China. *Soil Biol Biochem*. **134**: 1–14.

Zhao F Z, Wang J Y, Li Y, Xu X F, He L Y, Wang J, Ren C J, Guo Y X. 2022. Microbial functional genes driving the positive priming effect in forest soils along an elevation gradient. *Soil Biol Biochem*. **165**: 108498.

Zheng W, Zhao Z Y, Lv F L, Wang R Z, Wang Z H, Zhao Z Y, Li Z Y, Zhai B N. 2021. Assembly of abundant and rare bacterial and fungal sub-communities in different soil aggregate sizes in an apple orchard treated with cover crop and fertilizer. *Soil Biol Biochem*. **156**: 108222.

Zhong Z K, Li W J, Lu X Q, Gu Y Q, Wu S J, Shen Z Y, Han X H, Yang G H, Ren C J. 2020. Adaptive pathways of soil microorganisms to stoichiometric imbalances regulate microbial respiration following afforestation in the Loess Plateau, China. *Soil Biol Biochem*. **151**: 108048.

Zhou J Z, Ning D L. 2017. Stochastic community assembly: Does it matter in microbial ecology? *Microbiol Mol Biol Rev*. **81**: e00002-17.

Zhou X G, Hu Y T, Li H J, Sheng J D, Cheng J H, Zhao T T, Zhang Y M. 2024. Phosphorus addition increases stability and complexity of co-occurrence network of soil microbes in an artificial *Leymus chinensis* grassland. *Front Microbiol*. **15**: 1289022.

Zhu X F, Jackson R D, DeLucia E H, Tiedje J M, Liang C. 2020. The soil microbial carbon pump: From conceptual insights to empirical assessments. *Glob Change Biol*. **26**: 6032–6039.

Zhu Y F, Wang L P, Song X J, Li X X, Ma J, Chen F. 2023. Changes in abundant and rare microbial taxa that dominated the formation of soil carbon pool during short-term dryland-to-paddy conversion. *Carbon Res*. **2**: 26.